

EFFECTS AND PERFORMANCE OF SPECKLE NOISE REDUCTION FILTERS ON ACTIVE RADAR AND SAR IMAGES

M. Mansourpour^{a,*}, M.A. Rajabi^a, J.A.R. Blais^b

^a Dept. of Geomatics Eng., University of Tehran, Tehran, 14395-515 Iran - mansourpour@gmail.com, marajabi@ut.ac.ir

^b Dept. of Geomatics Eng., University of Calgary, Calgary, Alberta, T2N 1N4, Canada – blais@ucalgary.ca

KEY WORDS: RADAR, SAR Images, Noise, Speckle Filtering, Adaptive Filter, Signal to Noise Ratio

ABSTRACT:

Reduction of speckle noise is one of the most important processes to increase the quality of radar coherent images. Image variances or speckle is a granular noise that inherently exists in and degrades the quality of the active radar and SAR images. Before using active radar and SAR imageries, the very first step is to reduce the effect of Speckle noise. Most of speckle reduction techniques have been studied by researchers; however, there is no comprehensive method that takes all the constraints into consideration. Filtering is one of the common methods which is used to reduce the speckle noises. This paper compares six different speckle reduction filters quantitatively using both simulated and real imageries. The results have been presented by filtered images, statistical tables and diagrams. Finally, the best filter has been recommended based on the statistical and experimental results.

1. INTRODUCTION

According to Lillesand and Kiefer (2000) remote sensing is the science and art of obtaining information about an object, area, or phenomenon through the analysis of data acquired by a device that is not in contact with the object, area, or phenomenon under investigation. Based on the wavelength in which the system works, remote sensing is categorized into two different groups, i.e., optical and microwave. Optical remote sensing uses visible and infrared waves while microwave remote sensing uses radio waves.

As a microwave remote sensing, RADAR (Radio Detection And Ranging) sends out pulses of microwave electromagnetic radiation and measures the strength as well as time between the transmitted and reflected pulses to determine both the type of reflector and its distance from the transmitter (Raney, 1998). Different pulse intervals, different wavelengths (which ranges between less than 1 mm to 1 m), different geometry and polarizations can all be used to determine the roughness, geometry and moisture content of the earth surface (Henerson and Lewis, 1998). During the past two decades different satellites using RADAR sensors have been put into the orbit. SEASAT, SIR-A, SIR-B, SIR-C, ERS-1, ERS-2, ALMAZ, JERS-1, and RADARSAT are some of satellite missions which use RADAR technology.

A Synthetic Aperture Radar (SAR) system illuminates a scene with microwaves and records both the amplitude and the phase of the back-scattered radiation, making it a coherent imaging process. The received signal is sampled and converted into a digital image. The field recorded at pixel x , denoted $E(x)$, can be written as (InfoSAR Ltd, 2006)

$$E(x) = \sum_s a(s) \exp(i\varphi(s))h(s, x) \quad (1)$$

where the summation ranges over the scatterers, $a(s)$ and $\varphi(s)$ are respectively the amplitude and phase of the signal received from scatterer s , and h is the instrument (or point-spread) function. The value of h is near 1 when s is in or near the resolving cell corresponding to pixel x , and near zero otherwise. Assuming that h is translation-invariant (does not depend on x) then it can be written as a one-parameter function $h(s-x)$.

The detected field E is an array of complex numbers. The square of the modulus of the field at x is called the detected intensity at x ; the square-root of the intensity is called the envelope or the amplitude. This is not the same as the amplitude of the received signal because the received field is perturbed by the instrument function. The amplitude of the received signal, $a(s)$, is called the reflectivity, and its square is called the surface cross-section. Unfortunately, this is contaminated with speckle noise and the goal of all speckle noise reduction methods is to recover it.

In compare to optical remote sensing, radar imaging has some advantages. First, as an active system, it is a day/night data acquisition system. Second, considering the behaviour of electromagnetic waves in the range of RADAR wavelength, it can be seen that atmospheric characteristics such as cloud, light rain, haze, and smoke has little effect on the capability of RADAR data acquisition system. This makes RADAR as an all-weather remote sensing system. Last but not least, as the RADAR signals partially penetrate into soil and vegetation canopy, in addition to surface information, it can provide subsurface information too.

Inherent with all RADAR imageries is speckle noise which is nothing else but variation in backscatter from inhomogeneous cells. Speckle noise gives a grainy appearance to radar imageries. It reduces the image contrast which has a direct negative effect on texture based analysis of the imageries (Raney, 1998). Meanwhile, speckle noise also changes the spatial statistics of the underlying scene backscatter which in

* Corresponding author.

turn makes the classification of imageries a difficult task (Durand et al., 1987). Obviously, it is seen that to interpret RADAR imageries correctly one has to reduce (ideally remove!) the effect of speckle noise. However, as the speckle noise reduction/removal process changes the image as well, one should use proper filter to keep the image degradation minimum. This paper reviews the speckle noise reduction methods and among all studies the effect of mean, median, Lee-sigma, local region, Lee, Gamma-MAP, and Frost filters with different kernel sizes on the SAR imageries.

2. SPECKLE NOISE AND ITS REDUCTION

Radar waves can interfere constructively or destructively to produce light and dark pixels known as speckle noise. Speckle noise is commonly observed in radar (microwave or millimetre wave) sensing systems, although it may appear in any type of remotely sensed image utilizing coherent radiation. Like the light from a laser, the waves emitted by active sensors travel in phase and interact minimally on their way to the target area. After interaction with the target area, these waves are no longer in phase because of the different distances they travel from targets, or single versus multiple bounce scattering. Once out of phase, radar waves can interact to produce light and dark pixels known as speckle noise. Speckle noise in radar data is assumed to have multiplicative error model and must be reduced before the data can be utilized otherwise the noise is incorporated into and degrades the image quality. Ideally, speckle noise in radar images must be completely removed. However, in practice it can be reduced significantly. Reducing the effect of speckle noise permits both better discrimination of scene targets and easier automatic image segmentation.

Generally speaking, speckle noise can be reduced by multi-look processing or spatial filtering (Raney, 1998). While multi-look processing is usually done during data acquisition stage, speckle reduction by spatial filtering is performed on the image after it is acquired. No matter which method is used to reduce the effect of speckle noise, the ideal speckle reduction method preserves radiometric information, the edges between different areas and spatial signal variability, i.e., textural information. As this paper focuses on the effect of spatial filtering, interested readers can refer to Raney (1998) for more information on multi-look processing techniques.

The spatial filters are categorized into two different groups, i.e., non-adaptive and adaptive. Non-adaptive filters take the parameters of the whole image signal into consideration and leave out the local properties of the terrain backscatter or the nature of the sensor. These kinds of filters are not appropriate for non-stationary scene signal. Fast Fourier Transform (FFT) is an example of such filters. On the other hand, adaptive filters accommodate changes in local properties of the terrain backscatter as well as the nature of the sensor. In these types of filters, the speckle noise is considered as being stationary but the changes in the mean backscatters due to changes in the type of target are taken into consideration. Adaptive filters reduce speckles while preserving the edges (sharp contrast variation). These filters modify the image based on statistics extracted from the local environment of each pixel. Adaptive filter varies the contrast stretch for each pixel depending upon the Digital Number (DN) values in the surrounding moving kernel. Obviously, a filter that adapts the stretch to the region of interest (the area within the moving kernel) would produce a

better enhancement. Mean, median, Lee-Sigma, Local-Region, Lee, Gamma MAP, Frost are examples of such filters. Studying the effects of these filters are the subject of this paper therefore they are studied in a bit more detailed in the next section.

2.1 Speckle Filtering

As implicitly mentioned above, speckle filtering consists of moving a kernel over each pixel in the image and applying a mathematical calculation using the pixel values under the kernel and replacing the central pixel with the calculated value. The kernel is moved along the image one pixel at a time until the entire image has been covered. By applying the filter a smoothing effect is achieved and the visual appearance of the speckle is reduced.

2.1.1 Mean Filter: The Mean Filter is a simple one and does not remove the speckles but averages it into the data. Generally speaking, this is the least satisfactory method of speckle noise reduction as it results in loss of detail and resolution. However, it can be used for applications where resolution is not the first concern.

2.1.2 Median Filter: The Median filter is also a simple one and removes pulse or spike noises. Pulse functions of less than one-half of the moving kernel width are suppressed or eliminated but step functions or ramp functions are retained.

2.1.3 Lee-Sigma and Lee Filters: The Lee-Sigma and Lee filters utilize the statistical distribution of the DN values within the moving kernel to estimate the value of the pixel of interest. These two filters assume a Gaussian distribution for the noise in the image data. The Lee filter is based on the assumption that the mean and variance of the pixel of interest is equal to the local mean and variance of all pixels within the user-selected moving kernel. The formula used for the Lee filter is (Lee, 1981).

$$DN_{out} = [Mean] + K[DN_{in} - Mean] \quad (2)$$

where $Mean = \text{average of pixels in a moving window}$

$$K = \frac{Var(x)}{[Mean]^2 \sigma^2 + Var(x)}$$

and

$$Var(x) = \left(\frac{[Variance\ within\ window] + [Mean\ within\ window]^2}{[Sigma]^2 + 1} \right) - [Mean\ within\ window]^2$$

The Sigma filter is based on the probability of a Gaussian distribution. It is assumed that 95.5% of random samples are within a 2 standard deviation range. This noise suppression filter replaces the pixel of interest with the average of all DN values within the moving kernel that fall within the designated range (Lee, 1983).

2.1.4 Local Region Filter: The Local Region filter divides the moving kernel into eight regions based on angular position (North, South, East, West, NW, NE, SW, and SE). For each region, the variance is calculated, and then the algorithm

compares the variances of the regions surrounding the pixel of interest. The pixel of interest is replaced by the mean of all DN values within the region with the lowest variance.

2.1.5 Gamma-MAP Filter: The Maximum A Posteriori (MAP) filter is based on a multiplicative noise model with non-stationary mean and variance parameters. This filter assumes that the original DN value lies between the DN of the pixel of interest and the average DN of the moving kernel. Moreover, many speckle reduction filters assume a Gaussian distribution for the speckle noise. However, recent works have shown this to be invalid assumption. Natural vegetated areas have been shown to be more properly modelled as having a Gamma distributed cross section. The Gamma-Map algorithm incorporates this assumption and its exact formula is the following cubic equation (Frost et al., 1982):

$$\hat{I}^3 - \bar{I}\hat{I}^2 + \sigma(\hat{I} - DN) = 0 \quad (3)$$

where \hat{I} = sought value
 \bar{I} = local mean
 DN = input value
 σ = the original image variance.

The Gamma-MAP logic maximizes the a posteriori probability density function with respect to the original image. It combines both geometrical and statistical properties of the local area (Lopes et al., 1990). The filtering is controlled by both the variation coefficient and the geometrical ratio operators extended to the line detection (Touzi et al., 1998).

2.1.6 Frost Filter: The Frost filter replaces the pixel of interest with a weighted sum of the values within the $n \times n$ moving kernel. The weighting factors decrease with distance from the pixel of interest. The weighting factors increase for the central pixels as variance within the kernel increases. This filter assumes multiplicative noise and stationary noise statistics and follows the following formula:

$$DN = \sum_{n \times n} k \alpha e^{-\alpha|t|} \quad (4)$$

where $\alpha = (4/n\bar{\sigma}^2)(\sigma^2/\bar{I}^2)$
 k = normalization constant
 \bar{I} = local mean
 σ = local variance
 $\bar{\sigma}$ = image coefficient of variation value
 $|t| = |X - X_0| + |Y - Y_0|$, and
 n = moving kernel size (Lopes et al., 1990).

3. EXPERIMENTAL RESULTS

3.1 Simulated Imagery

The simulated imagery used for numerical experiment is a 227x167 pixel image with sharp edges (Figure 1). A uniformly distributed multiplicative noise with mean zero and variance 0.05 is added to the simulated imagery. To test the efficiency of the filters mentioned above, at the first step a 3x3 kernel is used for the filters. All of the filters are applied to the noise contaminated imagery. Figure 2 shows the noisy as well as the filtered image using a 3x3 kernel.



Figure1. The original simulated image

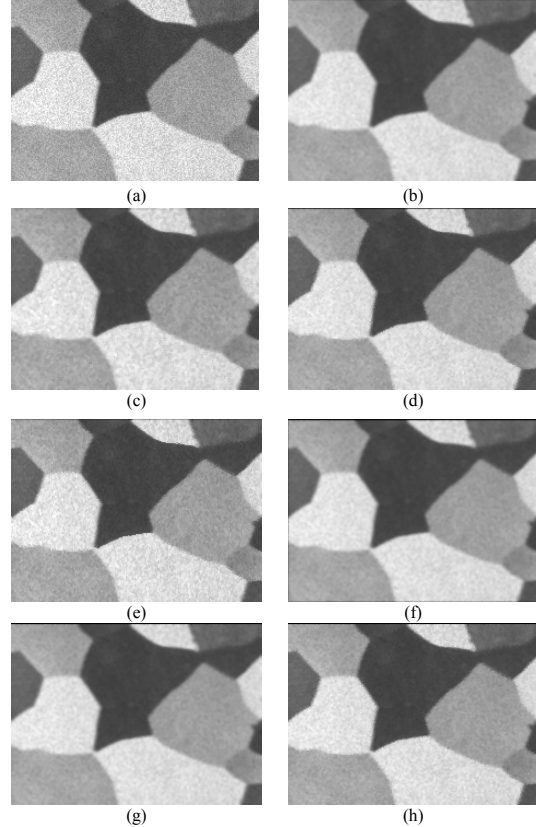


Figure 2. (a) Noisy image, (b) Mean, (c) Median, (d) Lee-Sigma, (e) Local Region, (f) Lee, (g) Gamma-MAP, and (h) Frost filters all with 3x3 kernel

In order to evaluate the result of filters quantitatively, the following three parameters are defined and calculated:

$$MSE = \frac{1}{K} \sum_{i=1}^K (\hat{S}_i - S_i) \quad (5)$$

where \hat{S} = noisy image
 S = original image
 K = image size

The standard signal-to-noise ratio (SNR) is not adequate to evaluate the noise suppression in the case of multiplicative noise. Instead, a common way to achieve this in coherent imaging is to calculate the signal-to-noise (S/MSE) ratio, defined as (Andrews and Hunt, 1977), (Starck et al., 1998):

$$SNR = 10 \log_{10} \left(\frac{\sum_{i=1}^K S_i^2 / \sum_{i=1}^K (\hat{S}_i - S_i)^2}{\sum_{i=1}^K S_i^2} \right) \quad (6)$$

This measure corresponds to the classical SNR in the case of additive noise. In SAR imaging one is interested in speckle noise suppression while at the same time preserving the edges and linear structures of the original image. Therefore, in addition to the above quantitative performance measures, another measure is also considered for edge preservation. More specifically, [32] and [33] have defined the parameter β as:

$$\beta = \frac{\Gamma(\Delta S - \Delta \hat{S}, \Delta \hat{S} - \Delta \bar{S})}{\sqrt{\Gamma(\Delta S - \Delta \bar{S}, \Delta S - \Delta \bar{S}) \Gamma(\Delta \hat{S} - \Delta \bar{S}, \Delta \hat{S} - \Delta \bar{S})}} \quad (7)$$

where ΔS and $\Delta \hat{S}$ are the high-pass filtered versions of S and \hat{S} respectively, obtained with a 3×3 pixel standard approximation of the Laplacian operator. The Laplacian high-pass filter used here for this purpose is as follows (Gonzalez and Woods, 2002):

$$\text{Laplacian Filter} = \begin{bmatrix} 0 & -1 & 0 \\ -1 & 4 & -1 \\ 0 & -1 & 0 \end{bmatrix} \quad (8)$$

Also the operator Γ denotes:

$$\Gamma(S_1, S_2) = \frac{\sum_{i=1}^K S_{1_i} \cdot S_{2_i}}{\sum_{i=1}^K S_{1_i} \cdot S_{2_i}} \quad (9)$$

The correlation measure β should be close to unity for an optimal effect of edge preservation. These three quantities are used to evaluate the speckle noise reduction method only when synthetic speckled image is used because the original noise-free image is needed.

For the filtered images all three quantities, i.e., MSE , SNR , and β are computed. The results are summarized in Table 3. It is seen that Gamma-Map, Frost, and Lee filters have the best results.

Filter Type	MSE	SNR	β
<i>Denoised Image</i>	135.0792	23.0073	0.5389
<i>Mean</i>	91.5039	24.6988	0.7754
<i>Median</i>	152.9449	22.4679	0.7062
<i>Lee-Sigma</i>	53.4389	27.0347	0.8631
<i>Local-Region</i>	150.9129	22.5260	0.6940
<i>Lee</i>	45.9487	27.6905	0.8645
<i>Gamma-MAP</i>	20.5826	31.1782	0.9599
<i>Frost</i>	31.1305	29.3814	0.9096

Table 3 Quantitative evaluation of the filters using a 3×3 kernel

To evaluate the effect of the kernel size on the performance of the filters, in the second step, the kernel size is extended to 5×5 and 7×7 pixels. The new kernels are used with just Gamma-Map, Frost, and Lee filters as these filters with the 3×3 kernel have shown good results. Tables 4 to 6 summarize the quantitative results of these tests.

MSE			
Kernel size / Filter Type	3×3	5×5	7×7
<i>Lee</i>	45.9487	69.6235	105.5413
<i>Gamma-MAP</i>	20.5826	23.1941	42.2455
<i>Frost</i>	31.1305	18.0322	17.0378

Table 4. MSE for the filter images with different kernel size

SNR			
Kernel Size / Filter Type	3×3	5×5	7×7
<i>Lee</i>	27.6905	25.8857	24.0790
<i>Gamma-MAP</i>	31.1782	30.6595	28.0554
<i>Frost</i>	29.3814	31.7528	31.9991

Table 5. SNR for the filtered images with different kernel size

β			
Kernel Size / Filter Type	3×3	5×5	7×7
<i>Lee</i>	0.8645	0.9307	0.9417
<i>Gamma-MAP</i>	0.9599	0.9728	0.9662
<i>Frost</i>	0.9096	0.9293	0.9186

Table 6. β for filtered images with different kernel size

These Tables show that by increasing the kernel size, Frost filter performs better than the other two filters from MSE and SNR point of view. However, from β point of view, Gamma-Map filter shows a better performance than the other two filters.

3.2 Real SAR Imagery

The real imagery used for numerical experimentation is a 340×360 pixel raw SAR image from Death Valley located at $116^\circ 30' 50'' N$ and $36^\circ 36' 30'' W$. The spatial resolution of this SAR image is 25 m and Figure 7.a shows it. All of the filters mentioned in the section 2 are applied to this image with different kernel size (Figure 7).

For the purpose of evaluating the performance of the filters quantitatively, two quantities of Mean and Standard Deviation (Std) are used. Based on these two quantities, the best performance filter is selected if the Mean of filtered image is close to the original image while the Std of filtered image has the minimum value.

Table 8 shows the numerical values of Mean and Std for the raw and filtered images with different kernel size. Moreover, the changes of these two parameters with respect to the corresponding values for the raw imagery as well as the value of Mean/Std value have been given too. Figure 9 and 10 show these results graphically. Figure 11 summarizes Figures 9 and 10 and shows Mean versus Std for both the raw and filtered images. Based on Table 8 and Figure 11, it is seen that Gamma-MAP, Frost and Lee filters with a 5×5 kernel have yielded the best results. On the other hand, in spite of the fact that Mean and Median filters reduce the value of Std, unfortunately, they dramatically change the value of Mean in compare to the Mean value for the raw image.

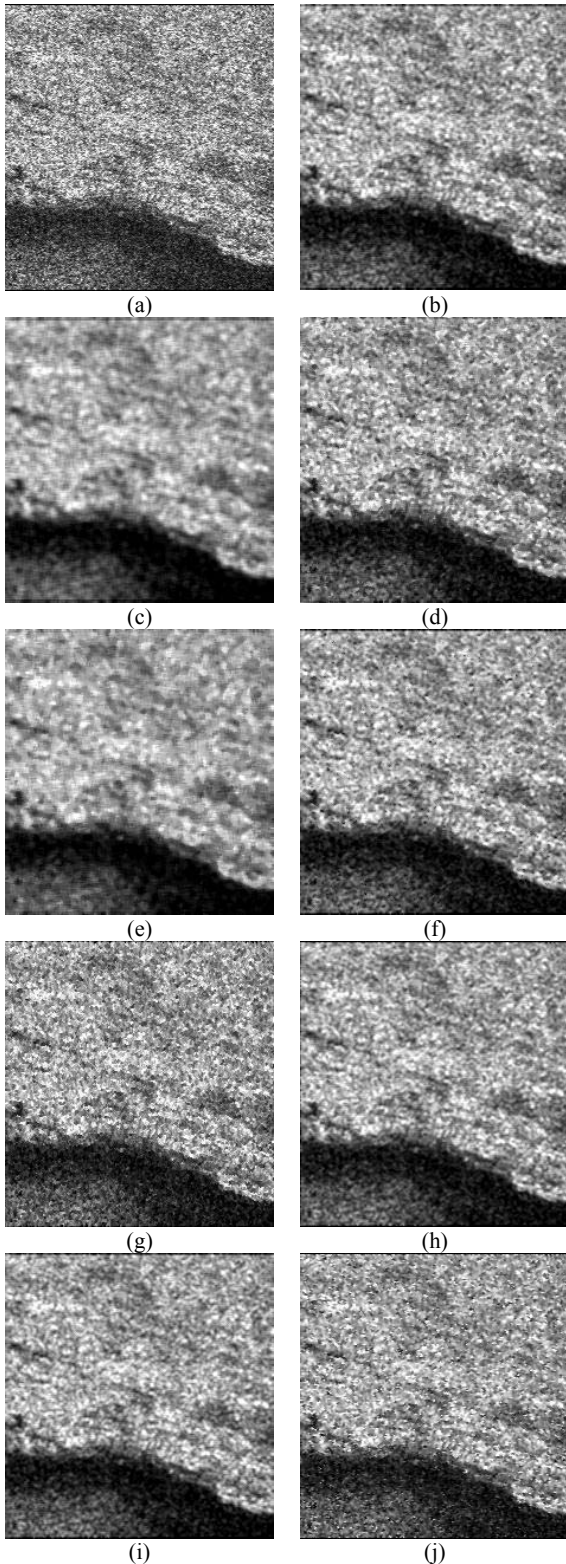


Figure 7. (a) The raw image, (b) and (c) Mean filter with 3x3 and 5x5 kernel s respectively, (d) and (e) Median filter with 3x3 and 5x5 kernels respectively, (f) Lee-Sigma filter, (g) local region filter, (h) Lee filter with 3x3 kernel, (i) Gamma-MAP filter, and (j) Frost filter all with 3x3 kernel

	Mean	Std	Mean/Std	Change in Mean	Change in Std
Raw	87.35	35.572	2.456	0	0
Mean 3x3	88.258	26.683	3.308	0.908	-8.889
Mean 5x5	88.078	24.451	3.602	0.728	-11.121
Median 3x3	85.665	27.255	3.143	-1.685	-8.317
Median 5x5	86.029	24.583	3.500	-1.321	-10.989
Lee-Sigma 3x3	86.82	27.279	3.183	-0.53	-8.293
Lee-Sigma 5x5	86.069	25.086	3.431	-1.281	-10.486
Local Region 3x3	86.369	29.48	2.930	-0.981	-6.092
Local Region 5x5	85.487	26.274	3.254	-1.863	-9.298
Frost 3x3	87.315	30.014	2.909	-0.035	-5.558
Frost 5x5	87.578	27.195	3.220	0.228	-8.377
Lee 3x3	87.431	27.662	3.161	0.081	-7.91
Lee 5x5	87.154	25.597	3.405	-0.196	-9.975
Gamma MAP 3x3	85.984	26.291	3.270	-1.366	-9.281
Gamma MAP 5x5	87.586	24.415	3.587	0.236	-11.157

Table 8. Mean, Std for raw and filtered images

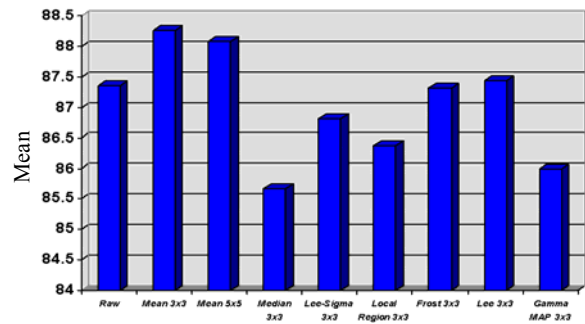


Figure 9. Mean values for raw and filtered images

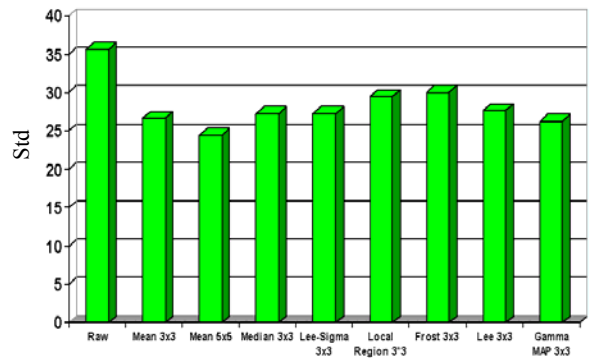


Figure 10. Std for raw and filtered images

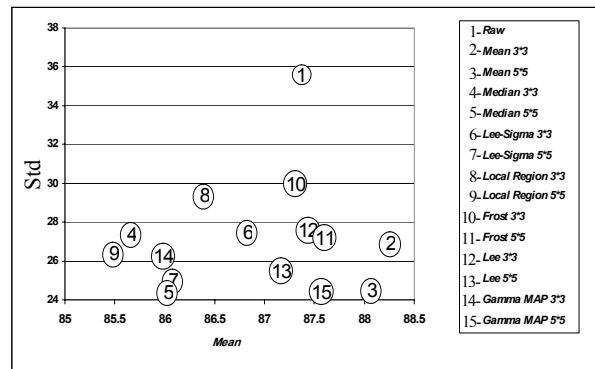


Figure 11. Mean versus Std for raw and filtered images

4. CONCLUSIONS AND REMARKS

Radar imageries are useful sources of information for roughness, geometry, and moisture content of the Earth surface. As an active, day/night, and all-weather remote sensing system, RADAR imageries can provide us information from both surface and subsurface of the Earth.

Inherent with RADAR imageries is speckle noise which gives a grainy appearance to the imageries. Speckle noise reduces the image contrast and has a negative effect on texture based analysis. Moreover, as speckle noise changes the spatial statistics of the images, it makes the classification process a difficult task to do. All of these show that to get information out of RADAR imageries one should first remove/reduce the effect of speckle noise.

Generally speaking there are two techniques of removing/reducing speckle noise, i.e., multi-look process and spatial filtering. Multi-look process is used at the data acquisition stage while spatial filtering is used after the data is stored. No matter which method is used to reduce/remove the speckle noise, they should preserve radiometric information, edge information and last but not least, spatial resolution. These are the conditions that any speckle noise reduction technique should meet.

Spatial filters are mainly categorized into two general groups, i.e., non-adaptive and adaptive filters. Non-adaptive filters are those which neglect the local properties of the terrain backscatter or nature of sensor. However, adaptive filters accommodate the change in the local properties of the terrain backscatter or the nature of sensor.

This paper reviewed the effect of applying six different adaptive filters on a simulated image as well as a real SAR imagery. To test the effect and performance of the filters, as the original and noisy image were available for the simulated image, one can use Mean Square Error, Signal to Noise ratio and β parameter (which shows the edge preserving strength of the filters). These three measures are able to evaluate the performance of filters quantitatively when both the original as well as noisy image are available. A good filter shows lower Mean Square Error, higher Signal to Noise Ratio, and a β closer to one.

However, in cases when the original image is not available, one can use only two parameters of Mean and Standard Deviation of noisy and filtered images to perform the filter assessment. A good filter has a lower difference between Means of the original and filtered images while preserving a low Standard Deviation for the filtered image.

In both simulated and real imageries it is seen that regardless of the kernel size, Mean, Median and Local Region filters perform poorly. This sounds a reasonable result as these filters do not take all the statistical characteristics of the image into consideration. In case of simulated imagery it is seen that the Gamma-MAP filter with a 3x3 kernel has the lowest MSE and highest SNR and β in compare to other filters with the same kernel. However, Frost filter with a 7x7 kernel has the lowest MSE and highest SNR. The numerical results show that Gamma-MAP filter performs much better for preserving the edge information.

In the case of real SAR imagery, the Gamma-MAP, Frost, and Lee filters with a 5x5 kernel show better results as the differences of their Means from the Mean of original image is low while they all have low Standard Deviation.

5. REFERENCES

- Andrews, H.C., Hunt, B.R., 1977. Digital Image Resstoration, Prentice-Hall, Engle-Wood Cliffs.
- Durand, M.J., Gimonet, B.J., Perbos, J.R., 1987. SAR Data Filtering for Classification. IEE, GE25 (5), 629-637.
- Frost, V.S., Stiles, J.A., Josephine, A., Shanmugan, K. S., and Holtzman, J.C., 1982. A Model for Radar Images and Its Application to Adaptive Digital Filtering of Multiplicative Noise. IEEE Transactions on Pattern Analysis and Machine Intelligence, Vol. PAMI-4, No. 2, March 1982.
- Gonzalez C., Woods, R.E., 2002. Digital Image Processing. Addison-Wesley Inc..
- Henerson, F.M., Lewis, A.J., 1998. Principles and Application of Imaging Radar. Volume1, John Wiley & Sons Inc., New York.
- InfoSAR Ltd, 2006. InfoPACK User Guide Version 1.0, <http://www.infosar.co.uk> (accessed 27 Jan. 2006).
- Lee, J.S., 1981. Speckle Analysis and Smoothing of Synthetic Aperture Radar Images. Computer Graphics and Image Processing, Vol. 17:24-32.
- Lee, J. S., 1983. Digital Image Smoothing and the Sigma Filter. Computer Vision, Graphics and Image Processing, 24, 255–269.
- Lopes A., Nezry, E., Touzi, R., and Laur, H., 1990. Maximum A Posteriori Speckle Filtering and First Order texture Models in SAR Images. International Geoscience and Remote Sensing Symposium (IGARSS).
- Raney, R.K., 1998. Radar Fundamentals: Technical Perspective. Chapter 2 in Principles and Applications of Imaging Radar, Manual of Remote Sensing, Third Edition, Volume 2, ASPRS, John Wiley and Sons Inc., Toronto.
- Starck, J.L., Murtagh, F., Bijaoui, A., 1998. Image Processing and Data Analysis, The multiscale approach. Cambridge University Press.
- Touzi, R., Lopes, A., Bousquet, P., 1998. A statistical and geometrical edge detector for SAR image. IEEE Transactions on Geoscience and Remote Sensing, Vol. 26, No. 6, pp. 764-773.
- Lillesand, M.T., Kiefer, R.W., 2000. Remote Sensing and Image Interpretation. Fourth Edition. John Wiley & Sons, New York.